

# Non-Equilibrium Heavy Flavored Hadron Yields from Chemical Equilibrium Strangeness-Rich QGP

Inga Kuznetsova and Johann Rafelski

Department of Physics, University of Arizona, Tucson, Arizona, 85721, USA

**Abstract.** The yields of heavy flavored hadrons emitted from strangeness-rich QGP are evaluated within chemical non-equilibrium statistical hadronization model, conserving strangeness, charm, and entropy yields at hadronization.

## 1. Introduction

A relatively large number of hadrons containing charm and bottom quarks are expected to be produced in heavy ion (AA) collisions at the Large Hadrons Collider (LHC). We are interested in how the high strangeness yield influences heavy and multi-heavy hadron yields (containing more than one heavy quark) [1]. Our work is differing from other recent studies [2, 3], since these assume that the hadron yields after hadronization are in chemical equilibrium. However, we form the charm  $c$  (and bottom  $b$ ) hadron yields in the statistical hadronization approach based on a given abundance of  $u, d, s$  quarks fixed by the bulk properties of a chemically equilibrated QGP phase. Since at LHC, and also RHIC, conservation of baryon number is not a vital element of the analysis, only entropy is preserved in the following, considering  $u, d, \bar{u}, \bar{d}$  yields.

Our approach is justified by the expectation that, in a fast break-up of the QGP formed at RHIC and LHC, the phase entropy and strangeness will be nearly conserved during the process of hadronization. If and when the volume doesn't change appreciably during hadronization, the entropy conservation determines values of hadron yields after hadronization. For QGP in chemical equilibrium, this implies that the final hadron yields are in general not in a chemical equilibrium. In this work, we will show how this influences the relative yields of heavy flavored particles in the final state. We will investigate in quantitative terms how such chemical non-equilibrium yields, in the conditions we explore well above the chemical equilibrium abundance, influence the expected yields of single, and multi-heavy flavor hadrons. We show that there are profound differences in hadron yields between the assumed hadron equilibrium and our approach.

## 2. Statistical hadronization model with conserved yields

During a fast transition between QGP (Q) and HG (H) phases strange  $i = s$  and heavier  $i = c$  and  $i = b$  quark flavor yields are preserved, as is the specific, per rapidity, hadronization volume, and in scaling limit, we also preserve the entropy per unit of rapidity [4]:

$$\frac{dN_i^H}{dy} = \frac{dN_i^Q}{dy}, \quad \frac{dS^H}{dy} = \frac{dS^Q}{dy}; \quad \frac{dV^Q}{dy} = \frac{dV^H}{dy}. \quad (1)$$

From now on we omit the upper index H. All parameters are for hadron side, unless there is an upper index Q.

The number of particles of type ‘ $i$ ’ with mass  $m_i$  per unit of rapidity is, in our approach, given by:

$$\frac{dN_i}{dy} = \Upsilon_i \frac{dV}{dy} n_i^{\text{eq}}. \quad (2)$$

Here,  $\Upsilon_i = \lambda_i \gamma_i$  is the particle  $i$  yield fugacity,  $dV/dy$  is the system volume associated with the unit of rapidity, and  $n_i^{\text{eq}}$  is a Boltzmann particles phase space density,

$$n_i^{\text{eq}} = g_i \int \frac{d^3p}{(2\pi)^3} \exp(-\sqrt{p^2 + m_i^2}/T) = g_i \frac{T m_i^2}{2\pi^2} K_2(m_i/T), \quad (3)$$

where  $g_i$  is the degeneracy factor,  $T$  is the temperature and  $p$  is the momentum.

The particle fugacity  $\lambda_i = e^{\mu_i/T}$  is associated with a conserved quantum number, of strangeness, charm, bottom, and baryon number:  $i = s, c, b$ . Antiparticles have negative chemical potential and thus  $\bar{\lambda} = \lambda^{-1}$ . The  $\lambda$  evolution during the reaction process is related to the changes in densities due to dynamics such as expansion. The phase space occupancy  $\gamma_i$  is the same for particles and antiparticles. Its value can change as a function of time even if the system does not expand, for it describes buildup of the particular particle species. For this reason  $\gamma_i$  very often changes rapidly, while  $\lambda$  is more constant. It is  $\gamma_i$  which is most sensitive to the time history of the reaction, except if full chemical equilibrium can be established, in which case  $\gamma_i \rightarrow 1$ .

The yields of hadrons after hadronization are given by Eq. (2), the unknown phase occupancies on hadron side for strangeness  $\gamma_s$  and heavy quarks  $\gamma_{c(b)}$  can be determined comparing quark yields in Q, H phases. The  $\gamma_s/\gamma_q$  ratio depends mostly on strangeness to entropy ratio  $s/S$  after hadronization, see fig.1, obtained using SHAREv.2.0 [5]. For LHC the expected ratio  $s/S = 0.038$  [6] at  $T = 140\text{--}180$  MeV which implies in the hadron phase  $\gamma_s/\gamma_q = 1.8\text{--}2$  [7].

## 3. Yields of heavy flavored hadrons

### 3.1. $D$ , $D_s$ , $B$ , $B_s$ meson yields

The predicted  $D$  and  $D_s$  mesons yield ratio  $D/D_s$  is shown in figure 2 on left, as a function of ratio  $\gamma_s/\gamma_q$  for  $T = 140, 160, 180$  MeV. A deviation of  $\gamma_s/\gamma_q$  from unity (from chemical equilibrium) leads to a noticeable change in the ratio  $D/D_s$ , which is

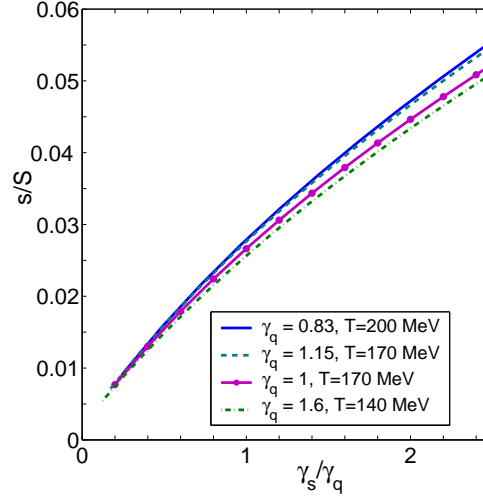


**Figure 1.** (color on line) Strangeness to entropy ratio,  $s/S$ , as a function of  $\gamma_s/\gamma_q$ . (solid line, blue) for  $T = 200$  MeV,  $S^H = S^Q \rightarrow \gamma_q = 0.83$ ; (dashed line, blue) for  $T = 170$  MeV,  $S^H = S^Q \rightarrow \gamma_q = 1.15$ ; (dash-dotted line, green) for  $T = 140$  MeV,  $S^H = S^Q \rightarrow \gamma_q = 1.6$ ; (dot marked solid, violet) for  $\gamma_q = 1, T = 170$ .

proportional to the inverse of  $\gamma_s/\gamma_q$  ratio. Ratio  $\gamma_s/\gamma_q$  grows with growth of strangeness to entropy ratio  $s/S$ . For LHC,  $s/S$  may reach a high value, and if  $s/S = 0.04$  then the ratio  $\gamma_s/\gamma_q$  is increased by about a factor 2 and  $D/D_s$  ratio is decreased by a factor 2 compared to the chemical equilibrium model. For  $B$ ,  $B_s$  mesons the results are the same as for  $D$ ,  $D_s$  mesons.

### 3.2. Heavy baryon yields

On the right, in figure 2, we show ratios  $cqq/cqs = (\Lambda_c + \Sigma_c)/\Xi_c$  and  $cqq/css = (\Lambda_c + \Sigma_c)/\Omega_c$  as a function of  $\gamma_s/\gamma_q$  for  $T = 200$  MeV (dash-dot line),  $T = 170$  MeV (solid line) and  $T = 140$  MeV (dashed line). The ratio  $cqq/cqs$  is inversely proportional to  $\gamma_s/\gamma_q$  ratio, similar as for  $D_s/D$  ratio. However,  $cqq/css \propto (\gamma_s/\gamma_q)^{-2}$ , further enhancing the effect of chemical non-equilibrium in QGP hadronization, with multistrange-charmed baryons produced at similar yield as nonstrange-charmed baryons.

### 3.3. Yields of hadrons with two heavy quarks

The yields of hadrons with several heavy quarks somewhat depend on hadronization condition, in particular on the reaction volume and on the total assumed charm yields. If we normalized yield of, for example, hidden charm mesons on  $N_c^2$  their yield only slightly depends on total charm multiplicity. The yields of hadrons with two heavy quarks are approximately proportional to  $1/(dV/dy)$  [8], because  $\gamma_c^H$  for heavy quarks is proportional to  $1/(dV/dy)$  [8], and only one power is cancelled by the proportionality to volume. The results we present are based on QGP reference state with  $dV/dy = 800 \text{ fm}^3$  at  $T = 200$  MeV, for  $s/S = 0.04$  and  $dV/dy = 600 \text{ fm}^3$  at  $T = 200$  MeV, for

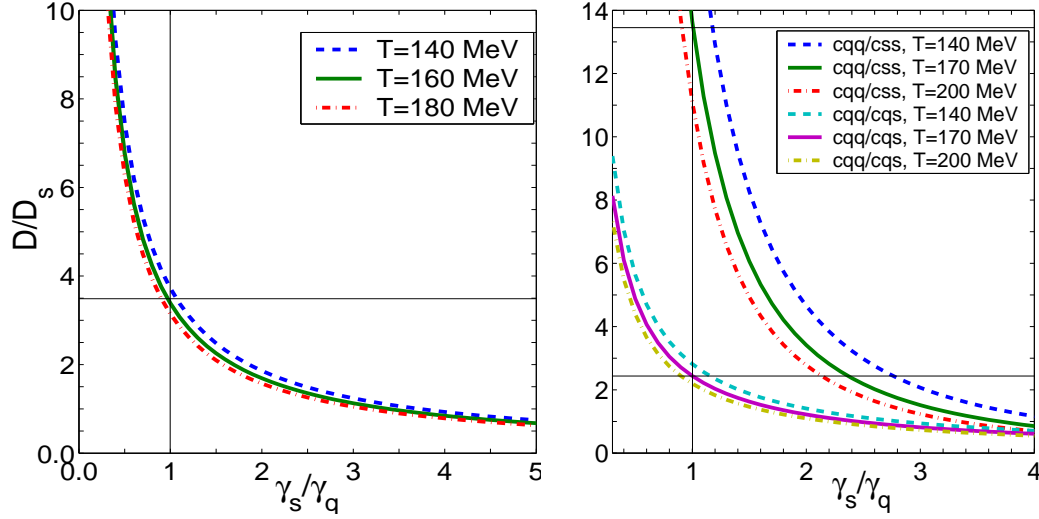


**Figure 2.** (color on line) Left:  $D/D_s$  ratio as a function of  $\gamma_s^H/\gamma_q^H$  for  $T = 140$  MeV (blue, dashed line),  $T = 160$  MeV (green, solid line) and  $T = 180$  MeV (red, dash-dot line). Right: The ratios  $cqq/cqs = (\Lambda_c + \Sigma_c)/\Xi_c$  (lower lines) and  $cqq/css = (\Lambda_c + \Sigma_c)/\Omega_c$  (upper lines) for  $T = 200$  MeV (dash-dot line),  $T = 170$  MeV (solid line) and  $T = 140$  MeV (dashed line).

$s/S = 0.03$ . Volume expands with drop in temperature preserving  $dS/dy$ . This corresponds considering entropy to a total final hadron particles multiplicity of about 5000 for  $s/S = 0.04$ .

In figure 3 we show the yield of hidden charm mesons  $c\bar{c}$  (sum over all states of  $c\bar{c}$ ) normalized by the square of charm multiplicity per rapidity  $N_c^2$  ( $N_c = 10$  for LHC and  $N_c = 3$  for RHIC) as a function of hadronization temperature  $T$ . We consider the cases  $s/S = 0.03$  and  $s/S = 0.04$  for LHC. We see that while the chemical equilibrium model predicts a yield falling with hadronization temperature  $T$ , the fixed  $s/S$  yield remains roughly independent of  $T$ . Remarkably, we see comparing right and left sides of figure 3 that in our model the expected yield of  $c\bar{c}$  mesons decreases with increasing specific strangeness and light quarks yields. The multiplicity of light quarks is also larger than in chemical equilibrium for  $T < 200$  MeV in the order to secure entropy conservation during hadronization. This new mechanism of charmonium suppression occurs due to competition with the yields of  $D$  and  $D_s$ .  $D$  and  $D_s$  in effect deplete the pool of available charmed quark pairs, and fewer hidden charm  $c\bar{c}$  mesons are formed. For larger  $T$ , right part of figure 3, the multiplicity of light quarks becomes smaller than equilibrium. This results in an enhancement of  $c\bar{c}$  yield in comparison with chemical equilibrium.

In figure 4 we quantify a more systematically this result. We compare the  $J/\Psi$  yield to the chemical equilibrium yield  $(J/\Psi)/(J/\Psi_{eq})$ , as a function of  $\gamma_s/\gamma_q$ , each line is at a fixed value  $\gamma_q$ . This ratio is:

$$\frac{J/\Psi}{J/\Psi_{eq}} = \frac{N_{hid}}{N_{hideq}} = \frac{\gamma_c^2}{\gamma_{ceq}^2}. \quad (4)$$

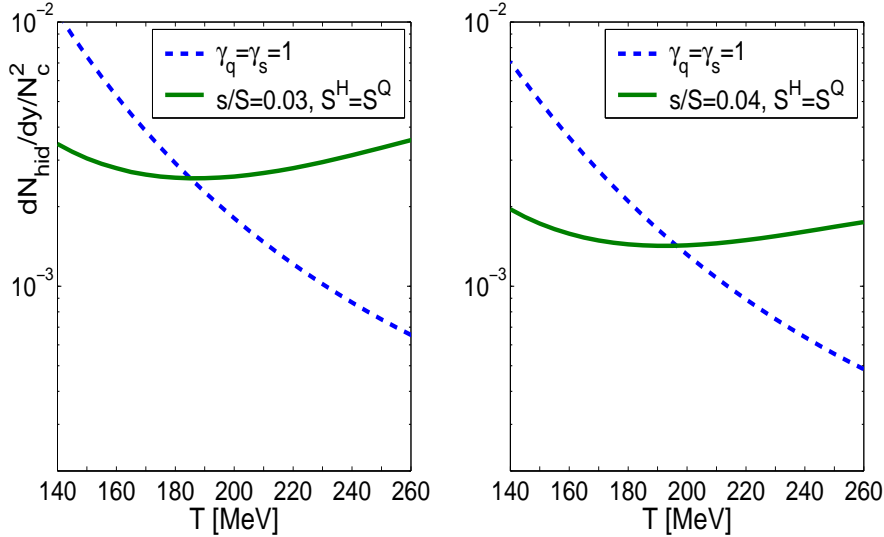


**Figure 3.**  $c\bar{c}/N_c^2$  relative yields as a function of hadronization temperature  $T$ . Dashed lines are for chemical equilibrium, solid lines for prescribed  $s/S$  in QGP. Left panel:  $dV/dy = 600 \text{ fm}^3$  at  $T = 200 \text{ MeV}$ , with  $s/S = 0.03$  for the nonequilibrium curve. Right panel:  $dV/dy = 800 \text{ fm}^3$  at  $T = 200 \text{ MeV}$  with  $s/S = 0.04$ .

$(J/\Psi)/(J/\Psi_{\text{eq}})$  always decreases when  $\gamma_s/\gamma_q$  increases, as we expect. We see that when we have small yields of light  $q, s$  quarks, we of course find  $J/\Psi/J/\Psi_{\text{eq}} > 1$ . This happens e.g. when hadronization is at  $T = 200 \text{ MeV}$ . In all other and ‘reasonable’ hadronization scenarios we find suppression  $(J/\Psi)/(J/\Psi_{\text{eq}}) < 1$ .

#### 4. Conclusions

We have considered the abundances of heavy flavor hadrons within the chemical non-equilibrium statistical hadronization model. We studied how the (relative) yields of strange and non-strange charmed mesons vary with a QGP produced fixed strangeness content. A considerable shift of the yield from non-strange  $D(B)$  to the strange  $D_s(B_s)$  and similar for strange-charmed baryons is expected for LHC since  $s/S$  may reach value about 0.04, which upon hadronization means  $\gamma_s/\gamma_q \cong 2$ .

Another important consequence of this result is that we find a relative suppression of the multi-heavy hadrons, including  $J/\Psi$ , for hadronization temperature lower than  $T = 200 \text{ MeV}$ , because strangeness and light quarks are above chemical equilibrium in HG after hadronization. We compared the yields to the expectations based on chemical equilibrium yields of light and strange quark pairs and found that the  $J/\Psi$  is suppressed, the mechanism being that abundantly produced light quark-charmed and strange-charmed hadrons deplete the pool of available charmed quarks.

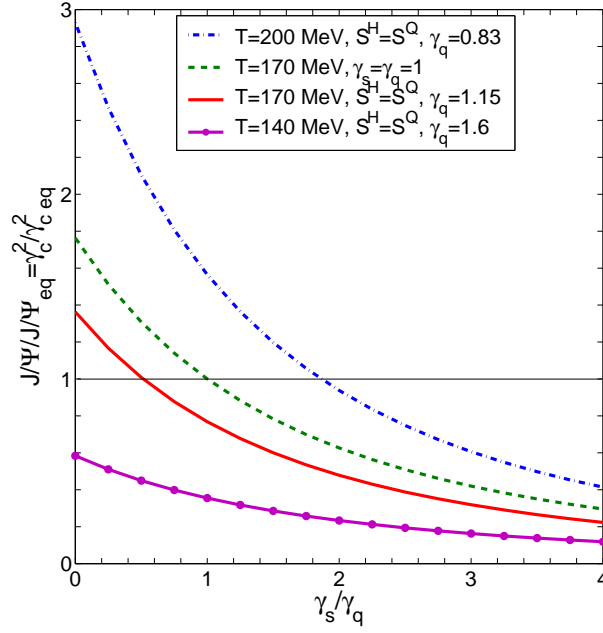


**Figure 4.** (Color on line) Ratio  $J/\Psi/J/\Psi_{eq} = \gamma_c^2/\gamma_{c eq}^2$  as a function of  $\gamma_s/\gamma_q$  at fixed value of  $\gamma_q$  and if required, entropy conservation. Shown are:  $T = 200$  MeV at  $\gamma_q = 0.83$  (dot-dash line, blue);  $T = 170$  MeV at  $\gamma_q = 1$  (dashed line, green) and at  $\gamma_q = 1.15$ , (solid line, red); at  $T = 140$  MeV,  $\gamma_q = 1.6$  (solid dotted line, purple)

*Acknowledgments* Work is supported by a grant from: the U.S. Department of Energy DE-FG02-04ER4131.

## 5. References

- [1] I. Kuznetsova and J. Rafelski, Eur. Phys. J. C **51** (2007) 113 [arXiv:hep-ph/0607203].
- [2] A. Andronic, P. Braun-Munzinger, K. Redlich and J. Stachel, Nucl. Phys. A **789** (2007) 334 [arXiv:nucl-th/0611023].
- [3] F. Becattini, Phys. Rev. Lett. **95**, 022301 (2005) [arXiv:hep-ph/0503239].
- [4] J. D. Bjorken, Phys. Rev. D **27**, 140 (1983).
- [5] G. Torrieri, S. Jeon, J. Letessier and J. Rafelski, Comput. Phys. Commun. **175** (2006) 635 [arXiv:nucl-th/0603026].  
G. Torrieri, S. Steinke, W. Broniowski, W. Florkowski, J. Letessier and J. Rafelski, Comput. Phys. Commun. **167**, 229 (2005) [arXiv:nucl-th/0404083].
- [6] J. Letessier and J. Rafelski, Phys. Rev. C **75**, 014905 (2007) [arXiv:nucl-th/0602047].
- [7] J. Rafelski and J. Letessier, Eur. Phys. J. C **45**, 61 (2006) [arXiv:hep-ph/0506140].
- [8] R. L. Thews, M. Schroedter and J. Rafelski, Phys. Rev. C **63**, 054905 (2001) [arXiv:hep-ph/0007323].